Origins of Life and Evolution of Biospheres (2006) 36: 363–379
DOI: 10.1007/s11084-006-9010-0

AB INITIO SIMULATIONS OF DESORPTION AND REACTIVITY OF GLYCINE AT A WATER-PYRITE INTERFACE AT "IRON-SULFUR WORLD" PREBIOTIC CONDITIONS

RODOLPHE POLLET[1,2,*], CHRISTIAN BOEHME[1,3] and DOMINIK MARX[1]
[1]*Lehrstuhl für Theoretische Chemie, Ruhr-Universität Bochum, 44780 Bochum, Germany;* [2]*Current and Permanent Address: Laboratoire Francis Perrin, CEA, 91191 Gif-sur-Yvette, France;* [3]*Current and Permanent Address: GWDG, Am Fassberg, 37077 Göttingen, Germany*
*(*author for correspondence, e-mail: rpollet@drecam.cea.fr)*

(Received 1 September 2005; accepted in revised form 25 January 2006)

Abstract. Glycine at the interface of a pyrite surface (001) FeS_2, and bulk water at high pressure and temperature conditions relevant to the "iron-sulfur world" scenario of the origin of life is investigated by theoretical means. Car-Parrinello molecular dynamics is used in order to study the desorption process of the zwitterionic form of this amino acid using two different adsorption modes, where either only one or both oxygens of the carboxylate group are anchored to surface iron atoms. It is found that the formation of stabilizing hydrogen bonds plays a key role in the detachment process, leading to longer retention times for the bidentate adsorption mode. In addition, the chemical reactivity of this heterogeneous system is probed by calculating the Fukui functions as site-specific reactivity indices. The most prominent targets for both nucleophilic and electrophilic reactions to occur are surface atoms, whereas the reactivity of glycine is only slightly affected upon anchoring.

Keywords: amino acids, Car-Parrinello molecular dynamics, hydrogen bonds, origins of life, pyrite surface

Introduction and Motivation

The emergence of complex biomolecules on earth, eventually resulting in the first forms of life, remains an intriguing puzzle to scientists across disciplines (Fry, 2000). Its explanation with the existence of a primordial soup has been advocated at least since the 1920s, with origins reaching back as far as Pasteur's experiments on broths at the end of the nineteenth century (Deamer and Fleischaker, 1994). The pioneering experiments of Miller (Miller, 1953; Bada and Lazcano, 2003) have established this hypothesis as one of the most prevalent paradigms since the 1950s. But in the 1990s another general class of scenarios, those involving mineral surface based reaction systems, see e.g. Refs. (Bernal, 1951; von Kiedrowski, 1996; Fry, 2000; Severin, 2000; Hazen, 2001; Dörr *et al.*, 2003; Saladino *et al.*, 2004), enjoys fresh impetus, partly in view of the stimulating work of Wächtershäuser (Wächtershäuser, 1988a; Wächtershäuser, 1992), which is however controversially discussed (de Duve and Miller, 1991; Bada and Lazcano, 2002; Wächtershäuser, 2002).

The basic premise of Wächtershäuser's so-called "iron-sulfur world" (ISW) hypothesis (Wächtershäuser, 1988a,b, 1990, 1992, 1994, 1998) is that the first biomolecules were synthesized at high pressure/high temperature thermo-dynamic conditions near sub-sea volcanoes, the so called hydrothermal vents. In this environment an abundance of iron-sulfur minerals is found, which serves the prebiotic chemistry in two important ways: (i) as an electron and energy source, and (ii) as a reaction environment which, via surface adsorption, *activates* and *concentrates* the reactants of the prebiotic chemistry, thus allowing for increasingly complex surface reaction systems. High pressures furthermore facilitate polymerization reactions, which are not favorable under the diluted primordialsoup conditions. This has been demonstrated by Huber and Wächtershäuser (Huber and Wächtershäuser, 1998) with the formation of dipeptides from amino acids in the presence of (Ni, Fe)S minerals at relatively mild conditions (2 bar and 100 °C), see also Ref. (Huber *et al.*, 2003). This key biochemical reaction is normally very unfavorable in aqueous solution, making this finding a major success of the ISW theory. Recently (Cody *et al.*, 2004) have concluded from CO insertion reactions that other iron-sulfide phases, like the much more prevalent pyrite, FeS_2, could also serve as catalysts.

Although the mechanism of the conversion of amino acids into dipeptides in the experiment of Huber and Wächtersh äuser is not yet understood, a sine qua non condition is obviously that the amino acids remain adsorbed on pyrite for a sufficient time span. This crucially depends not only on the chemical (i.e. electronic structure) and physical (e.g. morphology) properties of the surface itself, but also on solvent interactions involving the amino acids (i.e. competitive formation of hydrogen bonds *at the extreme ISW conditions*). Experimentally, however, the debate has been focused on the cationic or anionic nature of the pyrite surface at a given pH of the solution (Bebie *et al.*, 1998; Cody, 2004). A study of such a reaction system is furthermore complicated by a quite unusual environment, i.e. extremely hot and pressurized water at the water-pyrite interface. Fortunately, conditions which may be difficult to reproduce in a laboratory might easily be tackled "in silico". Thus, the calculation and analysis of microscopic quantities by computer simulation could, in principle, rationalize what de Duve and Miller call "random chemistry in two dimensions" (de Duve and Miller, 1991).

However, the computational literature on this subject is, at best, very scarce. Even outside this particular field, theoretical studies of amino acids adsorbed on surfaces are quite limited. Although density functional calculations of potential energy surfaces have been reported for glycine on copper (Nilsson and Pettersson, 2004), adenine on copper (Preuss *et al.*, 2005) and adenine on graphite (Ortmann *et al.*, 2005) surfaces, they typically focus on the surface-vacuum interface. A notable exception, although with a different aim, is a Car-Parrinello simulation of several amino acids including glycine on wet titanium oxide up to room temperature (Langel and Menken, 2003).

The water-pyrite interface has been studied as such since recently. Molecular dynamics computer simulations of the interface between water molecules and a

(001) pyrite surface (Philpott *et al.*, 2004) showed that water molecules do not desorb in the temperature range 225–425 °C. In addition, the molecules are found to be attached via their oxygen atom, O_{wat}, to an iron atom and via only one (Philpott *et al.*, 2004) or both (de Leeuw *et al.*, 2000) of the hydrogen atoms, H_{wat}, to sulfur atoms of this pyrite surface. The formation of a shorter and a longer hydrogen bond with surface sulfur atoms was also confirmed by *ab initio* molecular dynamics of monolayer systems (Stirling *et al.*, 2003b), which in addition established the existence of hydrogen bonds between the adsorbed water molecules themselves, see also Ref. (Stirling *et al.*, 2003a). These latter calculations also provided precious informations on the electronic structure of the water monolayer on pyrite by finding that the highest occupied molecular orbitals (HOMOs) are mainly the iron d_{xy}, d_{xz}, and d_{yz} orbitals, i.e. nonbonding t_{2g} orbitals, while the lowest unoccupied molecular orbitals (LUMOs) are mainly sulfur sp^3 orbitals with contributions of iron e_g orbitals. Interestingly, when the surface is dry, the latter contribution becomes predominant as d_{z^2} orbitals do not participate in binding the water molecules anymore. These observations tend to support the possibility of nucleophilic attacks involving the sulfur atoms *if the surface is wet.*

Here, we continue our simulation study of glycine at the water-pyrite interface at ISW conditions, see Ref. (Boehme and Marx, 2003) for a short preliminary note. Using the Car-Parrinello *ab initio* molecular dynamics method (Car and Parrinello, 1985; Marx and Hutter, 2000) allows us to analyze changes in electronic structure of both the (001) surface of FeS_2 and glycine as well as the interplay with dynamical effects such as solvation and most importantly hydrogen bonding. In particular we exploit the power of Fukui functions as local measures of chemical reactivity (Parr and Yang, 1989; Chermette, 1999; Vuilleumier and Sprik, 2001) in order to judge possible activation scenarios due to anchoring amino acids on pyrite surfaces at ISW conditions; see Ref. (Chattaraj, 2001) for a warning concerning the applicability of these descriptors to charge-controlled interactions. In addition we estimate roughly the retention time of glycine on the pyrite surface by analysing several trajectories of Car-Parrinello (CP) molecular dynamics (Car and Parrinello, 1985) simulations. The goal of our line of research is to offer eventually microscopic insights into the biophysical chemistry of such systems, which might be useful in order to scrutinize aspects of the ISW proposal.

Computational Approach

MODELING AND METHODOLOGY

All electronic structure calculations and *ab initio* simulations were performed within Kohn-Sham density functional theory using the PBE (Perdew *et al.*, 1996) exchange-correlation functional and the CPMD code (Marx and Hutter, 2000; CPMD, 2004). The closed-shell Kohn-Sham valence orbitals were expanded in

TABLE I

Calculated and experimental structural data of bulk pyrite

Method	Fe PP[a]	S PP[a]	Cut[b]	N_k^c	a^d	S-S[e]	Ref.[f]
PBE	US	US_d	25	64	5.404	2.191	
PBE	US_{sc}	US	25	64	5.403	2.184	
PBE	US_{sc}	US_d	25	64	5.411	2.195	
PBE	US_{sc}	US_d	25	8	5.410[g]	2.190	
PBE	US_{sc}	US_d	25	64	5.410[g]	2.194	
PBE	US_{sc}	US_d	25	216	5.410[g]	2.194	
exp.					5.416	2.161	Stevens *et al.* (1980)
exp.					5.407	2.135	Will *et al.* (1984)

[a] PP = pseudopotential, US = Vanderbilt ultrasoft (Vanderbilt, 1990; Laasonen *et al.*, 1993), suffix sc = semicore, suffix d = additional d-projector.
[b] Energy cutoff for plane wave expansion in Rydberg.
[c] Number of *k*-points.
[d] Cell constant in Å.
[e] S-S dumbbell bond length in Å.
[f] "This work" if no reference is specified.
[g] Kept constant.

a plane wave basis set in conjunction with Vanderbilt's ultrasoft pseudopotentials (Vanderbilt, 1990; Laasonen *et al.*, 1993) to describe the core electrons. Our benchmark calculations on bulk pyrite (see Table I) indeed show that a low energy cutoff of 25 Ry could reproduce the experimental cell parameter and the dumbbell-like S-S pair bond length. In these test calculations, semicore states for iron improved the convergence of the wave function optimization and an additional d-projector for sulfur increased the accuracy of the results so that both features were retained for all calculations.

An orthorhombic supercell of $\approx (10.8 \times 10.8 \times 18.9)$ Å was used. The (001) pyrite surface is represented by nine atomic layers (24 Fe and 48 S atoms), with the three lowest layers held fixed at optimized bulk positions. One glycine molecule and a lamella consisting of 35 water molecules was added which, at the thermostated temperature of 500 K, corresponds roughly to an expected pressure of ≈200 bar (i.e. 20 MPa).

Two *ab initio* molecular dynamics trajectories were launched for a monodentate adsorption mode and one for a bidentate setup. The former is characterized by attaching the carboxylate group of glycine to a surface iron atom via only one of the two oxygen atoms, whereas both bind to the surface in the bidentate configuration, see below for details. In all cases, the carboxyl group is deprotonated and the ammonia group is protonated resulting in an overall charge neutral system. In all three simulations, ISW conditions were reproduced by applying a temperature of 500 K via a Nosé-Hoover thermostat; the pressure of approximately 200 bar has been determined only very roughly by the number of water molecules and the available volume in the supercell. The mass of deuterium was assigned to hydrogen atoms in order to allow long time steps of 0.145 fs and 0.193 fs. In addition, the fictitious kinetic energy of the orbitals was controlled by a Nosé-Hoover thermostat as well in order to keep the electrons close to the instantaneous Born-Oppenheimer surface (Marx and Hutter, 2000).

Adsorption Scenarios

In aqueous solution, the stable form of glycine is the zwitterionic one. The free-energy changes associated to the intramolecular proton transfer of glycine in water (at room temperature) were probed by *ab initio* simulations (Leung and Rempe, 2005). Two distinct adsorption modes of zwitterionic glycine are considered in this study.

The first one is monodentate (see Figure 1, top row), implying that the carboxylate group of glycine is attached to a surface iron atom via only one oxygen atom (O_{gly}). This adsorption mode features also a weak hydrogen bond connecting the ammonium group of glycine to a sulfur atom (Boehme and Marx, 2003). The second adsorption mode is bidentate as depicted in the bottom row of Figure 1, as both oxygen atoms of glycine are attached to the surface. This latter mode is expected to be stronger than the monodentate one, although the later formation of a peptide bond in the presence of a second glycine molecule seems more difficult.

REACTIVITY MEASURES

In order to shed light on a possible activation of the adsorbed glycine molecules due to interactions with the surface, eight configurations were sampled from the various trajectories, four for each adsorption mode, and the corresponding electronic "Fukui functions" were calculated. These functions are generalizations of "frontier orbitals" known from molecular orbital theory within density functional theory. They probe locally the electronic response to small changes in the total number of electrons within a fixed nuclear configuration, and indeed reduce to the LUMO and HOMO densities in lowest order (Yang *et al.*, 1984), i.e. when the density and thus the Kohn-Sham orbitals are not relaxed upon this change. The Fukui functions as local electronic response parameters are defined as (Parr and Yang, 1989; Chermette, 1999; Vuilleumier and Sprik, 2001)

$$f^{\pm}(\mathbf{r}) = \lim_{N' \to N^{\pm}} \left. \frac{\partial \rho(\mathbf{r})}{\partial N'} \right|_{\mathbf{R}} \tag{1}$$

where $\rho(\mathbf{r})$ is the electron density at $\mathbf{r}$, $\mathbf{R}$ is the fixed ionic configuration, and N' is the fractional number of electrons approaching the integer number N from above and below for f^+ and f^-, respectively; these functions are normalized, $\int d\mathbf{r} f^{\pm}(\mathbf{r}) = 1$. Also called "site reactivity indices", they are used to identify

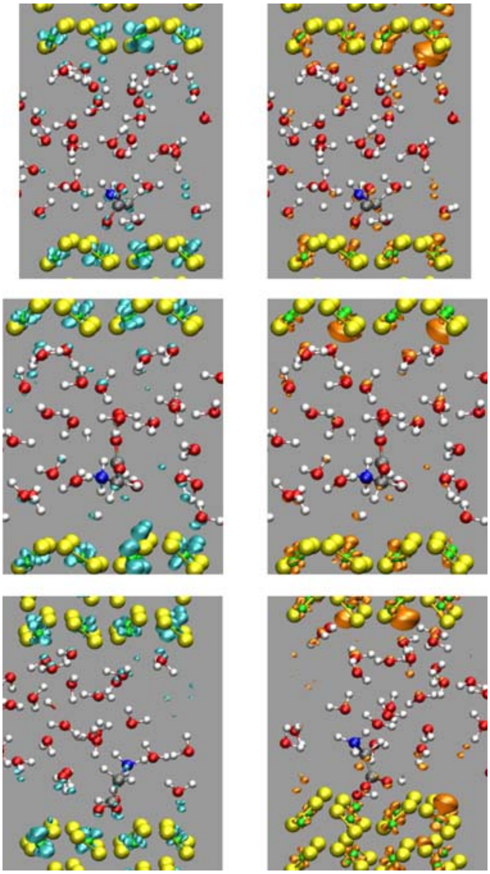

Figure 1. Fukui functions governing electrophilic attack, $f^-(\mathbf{r})$ (*left column*) and nucleophilic attack, $f^+(\mathbf{r})$ (*right column*) with glycine in the monodentate mode (*top row* = before desorption, *middle row* = after desorption) and in the bidentate mode (*bottom row*). Color code for Fe = green, S = yellow, C = black, N = blue, O = red, H = grey; f^- = cyan isosurface, f^+ = orange isosurface.

potential target locations for nucleophilic attack (cf. $f^+(\mathbf{r})$, i.e. when electrons are added locally at $\mathbf{r}$) or electrophilic attack (cf. $f^-(\mathbf{r})$, i.e. upon local electron removal). In fact, a Fukui function is just a normalized local softness (Chermette, 1999), the normalization factor being the (global) softness, which can be expressed in terms of ionization potential and electron affinity. Here, we use the efficient plane wave implementation of Fukui functions in CPMD (Marx and Hutter, 2000; CPMD, 2004) based on variational density functional perturbation theory by Vuilleumier and Sprik (Vuilleumier and Sprik, 2001). For technical reasons the Fukui functions were computed using dual-space Gaussian pseudopotentials (Hartwigsen *et al.*, 1998) with a cutoff of 100 Ry in conjunction with the BP86 (Perdew, 1986; Becke, 1988) functional.

Results and Discussion

MONODENTATE ADSORPTION MODE

Mechanism

Two independent *ab initio* simulations at ISW conditions were performed starting from the monodentate configuration (see Figure 1, top). For the first trajectory (Boehme and Marx, 2003), the desorption process of glycine occurred after about 1.5 ps, which can be followed in detail by plotting the Fe–O_{gly} distance (see Figure 2a).

The origin of the desorption of glycine can be correlated with the formation of a hydrogen bond between a solvent water and O_{gly} (resulting in a O_{gly}–O_{wat} distance of about 2.7 Å according to Figure 2a) which makes the Fe–O_{gly} interaction weaker. This event is analyzed in more detail in Figure 2(b) where the stretching and fluctuations of O_{wat}–H_{wat} covalent bond upon hydrogen bond donation as well as the concurrent decrease of the O_{gly}–O_{wat}–H_{wat} angle to the favorable value of less than 10° are apparent. It is interesting to note that this particular water molecule is actually adsorbed on the pyrite surface as well (its adsorption process can also be observed in Figure 2(a)), binding to an iron atom that belongs to the opposite side of the same groove (see Figure 3).

Finally, the desorption is achieved when the ammonium group unbinds as well from the surface, about 0.5 ps after the former detachment.

An alternative route to desorption is observed in the second trajectory, where the desorption starts with the breaking of the weak hydrogen bond that linked the ammonium group to one surface sulfur atom. The process can be observed in Figure 4, where the S–N and Fe–O_{gly} distances are monitored.

Whereas the detachment of the ammonium group occurs in one step around 2 ps, the carboxylate group is observed to re-attach to the surface. Thus, the desorption of the latter requires a second step setting in at $\approx$3 ps, which then allows the molecule to fully desorb from the surface. This two-step mechanism can actually be explained by two successive attacks of a single water molecule. Indeed, one of the water molecules forms during the simulation two successive hydrogen bonds between each of its hydrogen atoms and the oxygen atom of glycine attached to the surface (see Figures 5a, b, where very small O_{gly}–O_{wat}–H_{wat} angles were observed during each time window).

This analysis clearly shows that there is a correlation between the approach of the hydrogen atoms forming the hydrogen bonds and the two-step detachment of glycine. More precisely, some distinct features corresponding to long OH bonds are concurrent to increases of the Fe–O_{gly} distance, i.e. to a weakening of the interaction of the carboxylate group and the surface. It is assumed that the first hydrogen bond did not last long enough for the carboxylate group to desorb, whereas the second hydrogen bond attack gave rise to a more durable weakening.

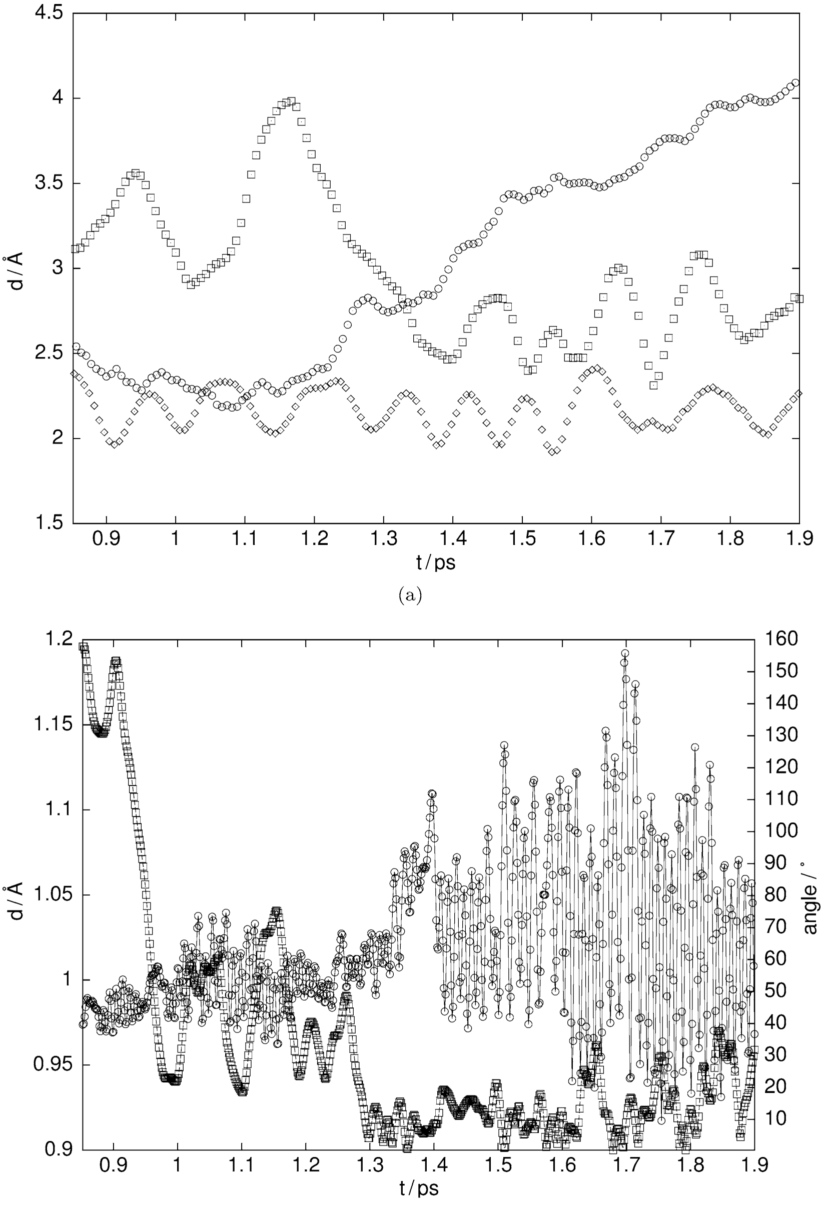

Figure 2. (a) Desorption process for the monodentate mode. Fe–O_{gly} distance: circle, O_{gly}–O_{wat} distance: square, S–O_{wat} distance: diamond. (b) Hydrogen bond attack responsible for the desorption process in the monodentate mode. O_{wat}–H_{wat} distance = circle, O_{gly}–O_{wat}-H_{wat} angle = square.

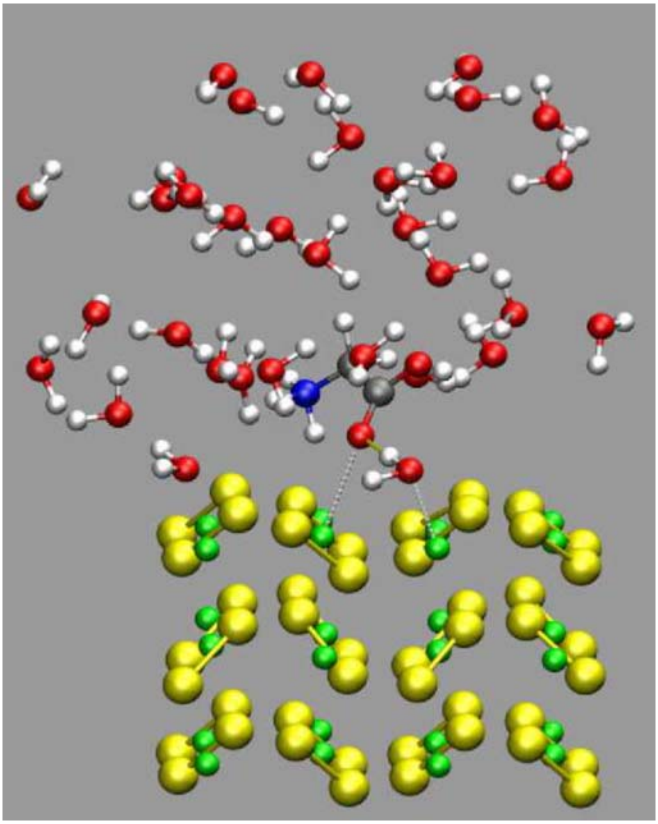

Figure 3. Hydrogen bond attack of an adsorbed water molecule onto one of the oxygen atoms of a monodentate adsorbed glycine.

ACTIVATION

The Fukui functions $f^{+}(\mathbf{r})$ and $f^{-}(\mathbf{r})$ as defined in Equation (1) should reveal, better than the corresponding LUMO and HOMO frontier orbitals, the influence of an adsorbed glycine on the reactivity of the pyrite surface. In addition, they should detect if some sites of glycine could be preferential targets for nucleophilic or electrophilic reactions. A general striking difference between all our computed Fukui functions and the corresponding frontier orbitals (not shown) is that the contributions to the latter are exclusively localized on the pyrite surface, while the Fukui functions are richer in that they are more delocalized showing additional, albeit small, contributions in the solvent and at the glycine molecule itself.

However, before we analyze the results obtained when glycine is present near the surface, it is suitable to describe the "bottom" face of the slab, which corresponds more or less to an unperturbed water-pyrite interface, albeit with fixed surface atoms (see the upper water-pyrite interfaces in the top and middle row panels of Figure 1).

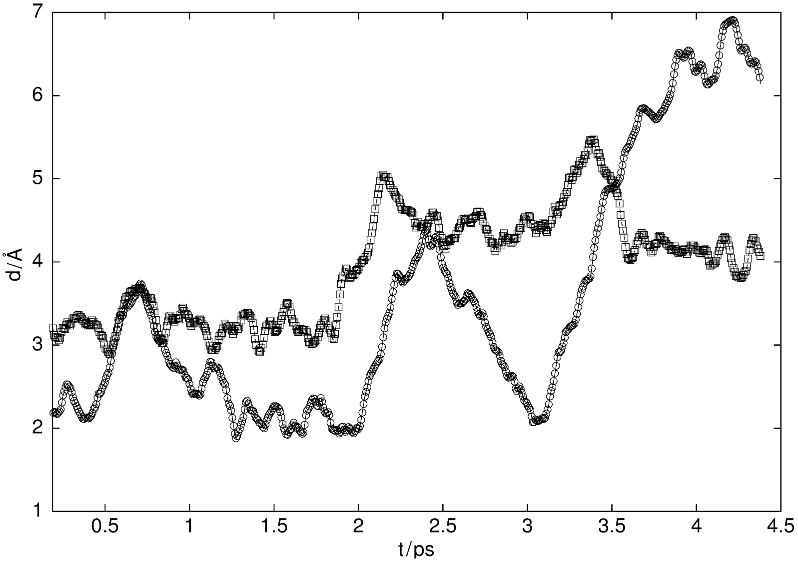

Figure 4. Two-step desorption process for the monodentate mode. S–N distance: square, Fe–O_{gly} distance: circle.

One notes that the electrophilic $f^{-}(\mathbf{r})$ Fukui functions depicted in the left column (as well as the corresponding HOMO orbitals, not shown) of this water-pyrite interface are dominated by iron t_{2g} orbitals contributions, possibly with additional ones located on surface sulfur atoms, i.e. on the ridge. This observation is only partially in accord with an earlier HOMO orbital analysis (Stirling *et al.*, 2003b) of pyrite covered with a water monolayer (i.e. one water molecule on each surface iron), where no contribution stemming from surface sulfur atoms is observed. On the contrary, a LUMO is found which is mainly composed of sulfur p orbitals whereas all our $f^{+}(\mathbf{r})$ Fukui functions (and LUMO orbitals) are mainly e_g iron orbitals contributions. This clearly means that in the present liquid-surface interface, at variance with the mono-layer setup, the water molecules are too far from the surface for a bond stabilizing the d_{z^2} orbitals to be formed. And indeed, the average Fe–O_{wat} distance is 2.28 Å (and not all adsorption sites are actually occupied), whereas a distance of 2.13 Å was found in the monolayer study (Stirling *et al.*, 2003b). Here, thermal motion is certainly a first contributing effect, as we have chosen a rather high temperature of 500 K according to ISW conditions, while in the monolayer the structure has been fully optimized which mimicks very low temperatures. More importantly, the present system features a bulk water-pyrite *interface* so that additional hydrogen bonds between bulk solvent molecules and directly adsorbed interfacial water, being of greater strength than surface S–H_{wat} interactions, tend to *destabilize* the water-surface interactions and thus drag water molecules away from the surface. Incidentally such effects were already mentioned

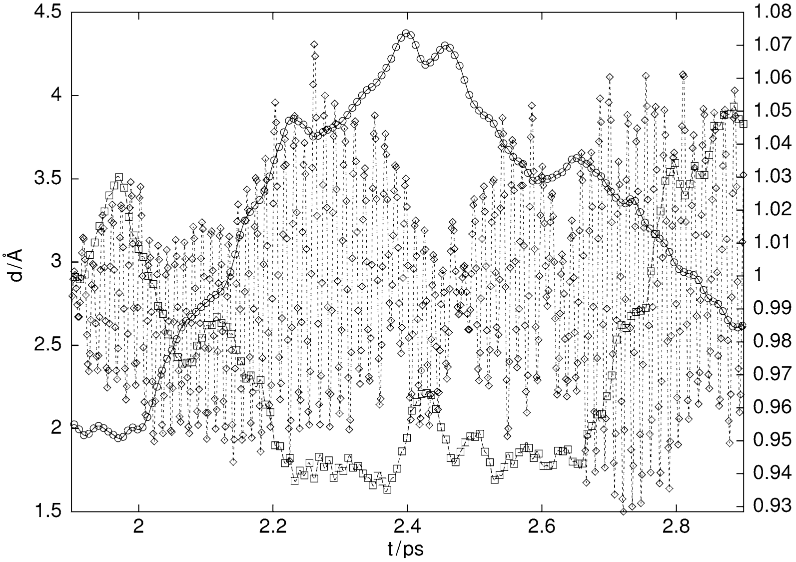

(a)

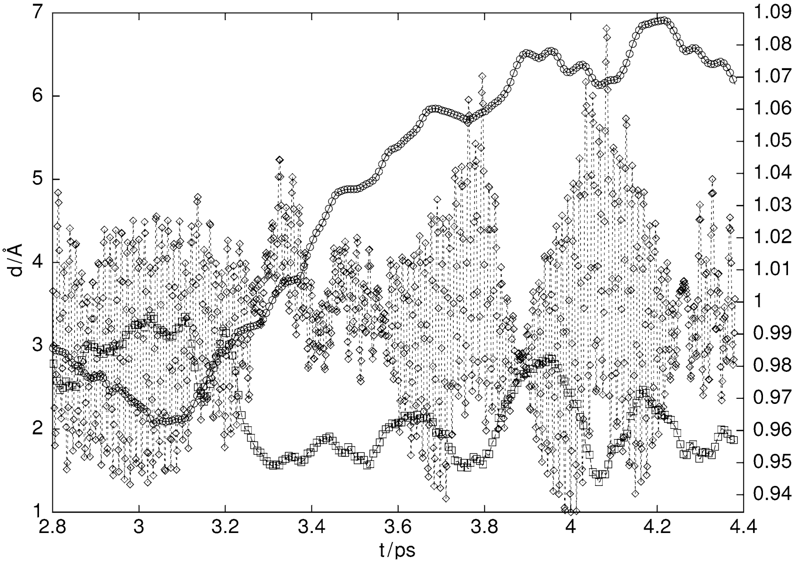

(b)

Figure 5. (a) First hydrogen bond attack within the two-step desorption process for the monodentate mode. Fe–O_{gly} distance = circle (*left axis*), H_{wat}–O_{gly} distance = square (*left axis*), H_{wat}–O_{wat} distance = diamond (*right axis*). (b) Second hydrogen bond attack within the two-step desorption process for the monodentate mode. Fe–O_{gly} distance = circle (*left axis*), H_{wat}–O_{gly} distance = square (*left axis*), H_{wat}–O_{wat} distance = diamond (*left axis*).

when an extra layer was added on top of the monolayer (Stirling *et al.*, 2003b). Concerning the Fe–O_{wat} distance, we also observe that any e_g orbital contribution to $f^+(\mathbf{r})$ (governing nucleophilic attacks) becomes outward-distorted whenever the (electronegative) oxygen atoms of those water molecules that surround the iron site are far from it in a given configuration.

Concerning the other face of the slab, Fukui functions were studied for both the adsorbed and the detached glycine molecule at the water-pyrite interface. In the monodentate absorption mode a configuration was sampled from the 4 ps trajectory after about 1.5 ps (see Figure 1, top row). Correspondingly, another configuration was sampled just after the desorption process has taken place at 3.6 ps (see Figure 1, middle row). Overall, the Fukui functions have barely changed in comparison to the opposite face, i.e. w.r.t. the "neat" water-pyrite interface. In Figure 1 (top left), the missing contribution on the surface sulfur atom is actually present in the corresponding HOMO. However, the shape of the $f^+(\mathbf{r})$ Fukui function (top right) is not outward-distorted anymore, indicating that the presence of glycine near the surface slightly inhibits nucleophilic attacks on iron atoms. Still, such a distortion was indeed observed for another desorbed configuration, extracted from the other monodentate trajectory. Even though these distortions seem less frequent around the glycine adsorption site it is interesting to note that the iron site where this outward contribution can be observed is located in an adjacent groove. From our observations, we can therefore conclude that the (nucleophilic) approach of another glycine molecule would probably lead to reactants in neighboring grooves. As for the glycine molecule, despite slightly bigger contributions to both $f^+(\mathbf{r})$ and $f^-(\mathbf{r})$ when it is still adsorbed on pyrite, these seem too small (if one compares with the contribution located on each solvent molecule for example) to prove any activation for this monodentate adsorption mode.

BIDENTATE ADSORPTION MODE

Mechanism

No full desorption occurred for the bidentate mode during the entire *ab initio* molecular dynamics simulation covering 9 ps. Still, each of the two oxygen atoms of the carboxylate group has temporarily detached itself from the pyrite surface, but not both at the same time (see Figure 6a for an example during our simulation).

The first detachment can be attributed to the weakening of the O_{gly}–Fe interaction due to the formation of a hydrogen bond between a neighboring water molecule and the detaching oxygen atom. This can be observed precisely in Figure 6b, where the O_{gly}–O_{wat}–H_{wat} angle gets lower than 10° and the O_{wat}–H_{wat} bond length increases just before the oxygen detaches. Taken together, this clearly shows that the dynamics of hydrogen bonds between water and glycine are crucial in the desorption process. However, it seems that glycine is more firmly attached to the surface in the bidentate mode.

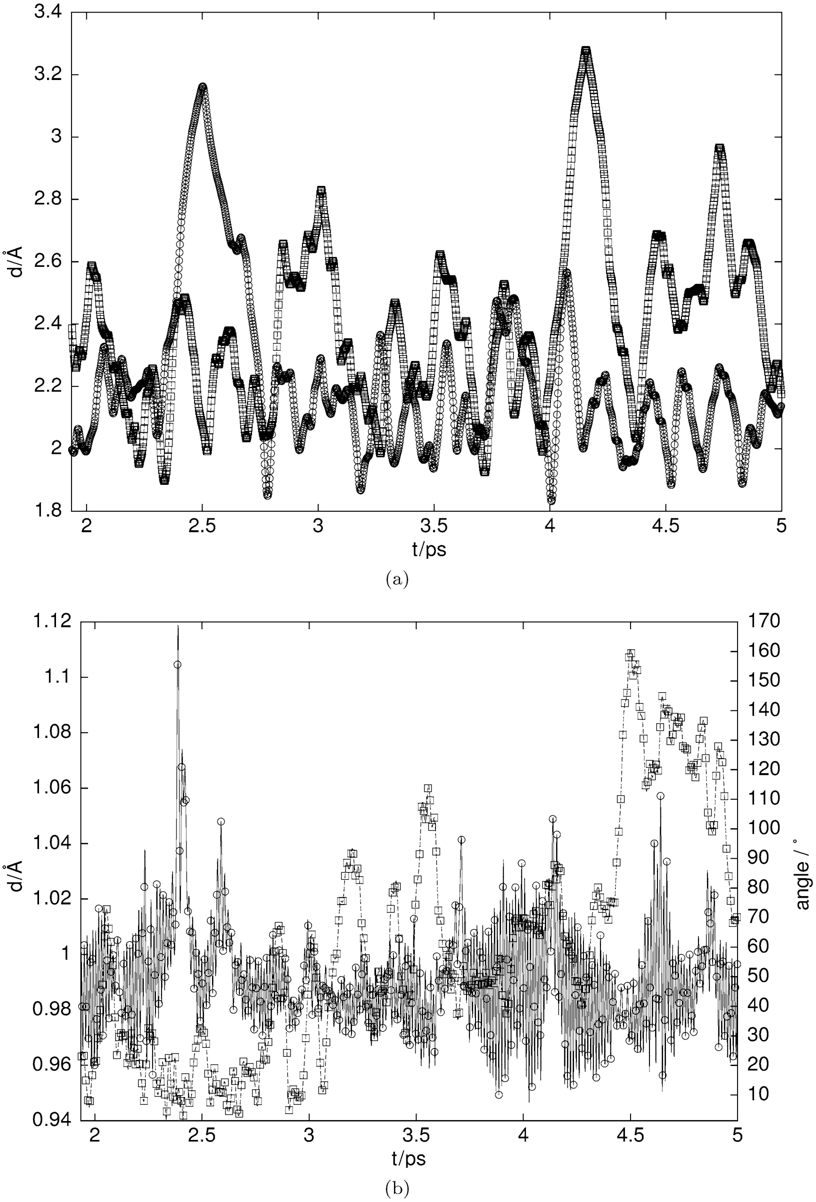

(a)

(b)

Figure 6. (a) Transient detachments for the bidentate mode = Fe–$O_{gly,1}$ and Fe–$O_{gly,2}$ (where $O_{gly,1}$ and $O_{gly,2}$ are the two oxygen atoms of the carboxylate group of glycine) distances. (b) Evidences of the hydrogen bond attack of a solvent water molecule onto one of the oxygen atoms = O_{wat}–H_{wat} distance = circle, O_{wat}–H_{wat}–O_{gly} angle = square.

Before we analyze the possible activation of glycine, we want to emphasize that in the context of ISW scenarios, such a conformation is nevertheless a worse candidate for the formation of diglycine compared to the monodentate mode because the $-NH_3^+$ group is screened by solvating water molecules. Furthermore the dynamical flexibility of the latter lowers the reaction probability with respect to the monodentate mode, where both reacting groups assume rather fixed positions in space. Interestingly, a possible interconversion between the two modes could be initiated in the bidentate mode by the detachment of a single oxygen atom while the remaining one would serve as a pivot point.

Activation
A configuration was extracted from the trajectory after 5.7 ps where both oxygen atoms of the carboxylate group were anchored to the pyrite surface. The corresponding $f^-(\mathbf{r})$ and $f^+(\mathbf{r})$ Fukui functions are shown in Figure 1 (see bottom row). In comparison with the monodentate mode, the activity of the carbon atom of the carboxylate group seems slightly increased, as expected. As for the (not shown) monodentate-adsorbed configuration previously mentioned, we find that one of the iron atoms located in an adjacent groove exhibits a large outward-distorted contribution, and therefore becomes the preferential target for nucleophilic attacks (possibly another adsorption, see previous discussion). Interestingly, for another configuration (extracted after 0.85 ps), we observe such a distortion on an iron site located in the same groove, which paves the way for an alternate approach of another glycine.

Conclusions and Outlook

Car-Parrinello molecular dynamics simulations indicate that the retention time of a zwitterionic glycine molecule at the ideal (001) surface of pyrite at “iron-sulfur world” conditions, i.e. in the presence of hot and pressurized bulk water, greatly depends on its adsorption mode. When the glycine molecule is attached to the surface via a single oxygen atom, i.e. in the monodentate adsorption mode, desorption appears to be a very efficient and thus fast process. This can be correlated with preferential formation of hydrogen bonds with surrounding water molecules, which appear to greatly stabilize the detaching amino acid in its zwitterionic state. On the other hand when the glycine molecule is attached to the surface via both oxygen atoms of its carboxylate group, i.e. in the bidentate mode, such hydrogen bonds need to be formed simultaneously with both atoms for the desorption to be activated. Alternatively, such stabilizing hydrogen bonds could be formed one after the other, thus resulting in a slower detachment process. In the present simulation, we only observed temporary detachments of *one* carboxylate oxygen, and therefore no full desorption of glycine in the bidentate mode. In general, it is found that the detailed hydrogen bond dynamics play a pivotal role in determining the retention and desorption properties of small peptides at the water-pyrite interface. As for the chemical activity of the glycine molecule, the calculation and analysis of Fukui functions revealed that its reactivity is only slightly affected by adsorbing it on the surface. The surface itself remains the most prominent target for both nucleophilic and electrophilic reactions to occur, in particular the iron atoms. However, the activity of the carboxylate carbon of glycine is slightly increased in the bidentate adsorption mode, compared to the monodentate one. Therefore the reaction probability with respect to a neighboring second glycine molecule might be sufficiently high if the spatial orientation is favorable.

An alternative route to immobilize an amino acid on the surface would be to add a COS group to glycine, in order to fix the resulting carbothioacid onto the pyrite surface (Huber and Wächtershäuser, 1998). Furthermore, surface defects are expected to strongly impact on the adsorption mode of glycine on pyrite. Thus, the breaking-up of bonds in the sulfur-sulfur dimers, variations of the coordination number of iron atoms, and the creation of defects in general should be considered in the future. Stimulated by the present results, work along these lines is currently in progress.

Acknowledgments

We are grateful to Eddi Schreiner and Nisanth Nair for fruitful discussions and to Rodolphe Vuilleumier for having shared his experience with the computation of Fukui functions. We thank SSCK (Karlsruhe), Rechnerverbund-NRW, and BOVILAB@RUB (Bochum) for providing computational resources and we gratefully acknowledge DFG (MA 1547/7) and FCI for partial financial support.

References

Bada, J. L. and Lazcano, A.: 2002, Origin of Life-Some Like It Hot, But Not the First Biomolecules, *Science* **296**(5575), 1982–1983.

Bada, J. L. and Lazcano, A.: 2003. Prebiotic Soup-Revisiting the Miller Experiment, *Science* **300**(5620), 745–746.

Bebie, J., Schoonen, M. A. A., Fuhrman, M. and Strongin, D. R.: 1998, Surface Charge Development on Transition Metal Sulfides: An electrokinetic study, *Geochim. Cosmochim. Acta.* **62**(4), 633–642.

Becke, A. D.: 1988, Density-Functional Exchange-Energy Approximation with Correct Asymptotic-behavior, *Phys. Rev. A* **38**(6), 3098–3100.

Bernal, J. D. ed.: 1951, The Physical Basis of Life. Routledge and Kegan Paul Ltd., London. See in particular pp. 33.

Boehme, C. and Marx, D.: 2003, Glycine on a Wet Pyrite Surface at Extreme Conditions, *J. Am. Chem. Soc. (Communication to the Editor)* **125**, 13362–13363.

Car, R. and Parrinello, M.: 1985, Unified Approach for Molecular-Dynamics and Density-Functional Theory, *Phys. Rev. Lett.* **55**(22), 2471–2474.

Chattaraj, P. K.: 2001, Chemical Reactivity and Selectivity: Local HSAB Principle Versus Frontier Orbital Theory, *J. Phys. Chem. A* **105**(2), 511–513.

Chermette, H.: 1999, Chemical Reactivity Indexes in Density Functional Theory, *J. Comput. Chem.* **20**(1), 129–154.

Cody, G. D.: 2004, Transition Metal Sulfides and the Origins of Metabolism, *Annu. Rev. Planet. Sci.* **32**, 569–599.

Cody, G. D., Boctor, N. Z., Brandes, J. A., Filley, T. R., Hazen, R. M. and Yoder, H. S. J.: 2004, Assaying the Catalytic Potential of Transition Metal Sulfides for Abiotic Carbon Fixation, *Geochim. Cosmochim. Acta.* **68**(10), 2185–2196.

de Duve, C. and Miller, S. L.: 1991, 2-Dimensional Life, *Proc. Natl. Acad. Sci. USA* **88**(22), 10014–10017.

de Leeuw, N. H., Parker, S. C., Sithole, H. M. and Ngoepe, P. E.: 2000, Modeling the Surface Structure and Reactivity of Pyrite: Introducing a Potential Model for FeS2, *J. Phys. Chem. B* **104**(33), 7969–7976.

Deamer, D. W. and Fleischaker, G. R. (eds.): 1994, *Origins of Life.* Bartlett Publishers, Boston.

Dörr, M., KäBbohrer, J., Grunert, R., Kreisel, G., Brand, W. A., Werner, R. A., Geilmann, H., Apfel, C., Robl, C. and Weigand, W.: 2003, A Possible Prebiotic Formation of Ammonia from Dinitrogen on Iron Sulfide Surfaces, *Angew. Chem. Int. Ed.* **42**, 1540–1543.

Fry, I.: 2000, *The Emergence of Life on Earth*, Rutgers UP, New Brunswick.

Hartwigsen, C., Goedecker, S. and Hutter, J.: 1998, Relativistic Separable Dual-Space Gaussian Pseudopotentials from H to Rn. *Phys. Rev. B* **58**(7), 3641–3662.

Hazen, R. M.: 2001, *Life's Rocky Start, Scientifc American*, April: 76–85.

Huber, C., Eisenreich, W., Hecht, S. and Wächtershäuser, G.: 2003, A Possible Primordial Peptide Cycle, *Science* **301**(5635), 938–940.

Huber, C. and Wächtershäuser, G.: 1998, Peptides by Activation of Amino Acids with CO on (Ni, Fe)S Surfaces: Implications for the Origin of Life, *Science* **281**(5377), 670–672.

Laasonen, K., Pasquarello, A., Car, R., Lee, C. and Vanderbilt, D.: 1993, Car-Parrinello Molecular-Dynamics with Vanderbilt Ultrasoft Pseudopotentials, *Phys. Rev. B* **47**(16), 10142–10143.

Langel, W. and Menken, L.: 2003, Simulation of the Interface Between Titanium Oxide and Amino Acids in Solution by First Principles MD, *Surf. Sci.* **538**, 1–9.

Leung, K. and Rempe, S. B.: 2005, *ab initio* Molecular Dynamics Study of Glycine Intramolecular Proton Transfer in Water, *J. Chem. Phys.* **122**, 184506, 1–12.

Marx, D. and Hutter, J.: 2000, *ab initio* molecular dynamics: Theory and implementation, in Grotendorst, J. (ed.), *Modern Methods and Algorithms of Quantum Chemistry*, pp. 301–449, NIC, Jülich. for downloads see www.theochem.rub.de/go/cprev.html.

Miller, S. L.: 1953, A Production of Amino Acids Under Possible Primitive Earth Conditions, *Science* **117**, 528–592.

Nilsson, A. and Pettersson, L. G. M.: 2004, Chemical Bonding on Surfaces Probed by X-ray Emission Spectroscopy and Density Functional Theory, *Surf. Sci. Rep.* **55**, 49–167.

Ortmann, F., Schmidt, W. G. and Bechstedt, F.: 2005, Attracted by Long-Range Electron Correlation: Adenine on Graphite, *Phys. Rev. Lett.* **95**, 186101–1-186101–4.

Parr, R. G. and Yang, W.: 1989, *Density-Functional Theory of Atoms and Molecules*, Oxford University Press, New York.

Perdew, J. P.: 1986, Density-Functional Approximation for the Correlation-Energy of the Inhomogeneous Electron-Gas, *Phys. Rev. B* **33**(12), 8822–8824.

Perdew, J. P., Burke, K. and Ernzerhof, M.: 1996, Generalized Gradient Approximation Made Simple, *Phys. Rev. Lett.* **77**(18), 3865–3868. Erratum: 1997, 78, 1396.

Philpott, M. R., Goliney, I. Y. and Lin, T. T.: 2004, Molecular Dynamics Simulation of Water in a Contact with an Iron Pyrite FeS2 Surface, *J. Chem. Phys.* **120**(4), 1943–1950.

Preuss, M., Schmidt, W. G. and Bechstedt, F.: 2005, Coulombic Amino Group-Metal Bonding: Adsorption of Adenine on Cu(110), *Phys. Rev. Lett.* **94**, 236102–1-236102–4.

Saladino, R., Crestini, C., Ciambecchini, U., Ciciriello, F., Costanzo, G. and Di Mauro, E.: 2004, Synthesis and Degradation of Nucleobases and Nucleic Acids by Formamide in the Presence of Montmorillonites, *Chem. Bio. Chem.* **5**, 1558–1556.

Severin, K.: 2000, Hot Stones or Cold Soup? *Angew. Chem. Int. Ed.* **39**, 3589–3590.

Stevens, E. D., DeLucia, M. L. and Coppens, P.: 1980, Experimental-Observation of the Effect of Crystal-Field Splitting on the Electron-Density Distribution of Iron Pyrite. *Inorg. Chem.* **19**(4), 813–820.

Stirling, A., Bernasconi, M. and Parrinello, M.: 2003a, *ab initio* Simulation of H_2S Adsorption on the (100) Surface of Pyrite. *J. Chem. Phys.* **119**, 4934–4939.

Stirling, A., Bernasconi, M. and Parrinello, M.: 2003b, *ab initio* Simulation of Water Interaction with the (100) Surface of Pyrite, *J. Chem. Phys.* **118**, 8917–8926.

CPMD (2004): Hutter J. *et al.*, Copyright: IBM Corp 1990–2004, MPI für Festkörperforschung Stuttgart 1997–2001.

Vanderbilt, D.: 1990, Soft Self-Consistent Pseudopotentials in a Generalized Eigenvalue Formalism, *Phys. Rev. B* **41**(11), 7892–7895.

von Kiedrowski, G.: 1996, Origins of life–Primordial soup or crêpes? *Nature* **381**, 20–21.

Vuilleumier, R. and Sprik, M.: 2001, Electronic Properties of Hard and Soft Ions in Solution: Aqueous Na^+ and Ag^+ Compared, *J. Chem. Phys.* **115**(8), 3454–3468.

Wächtershäuser, G.: 1988a, Before Enzymes and Templates – Theory of Surface Metabolism, *Microbiol. Rev.* **52**(4), 452–484.

Wächtershäuser, G.: 1988b, Pyrite Formation, the 1st Energy-Source for Life – A Hypothesis, *Syst. Appl. Microbiol.* **10**(3), 207–210.

Wächtershäuser, G.: 1990, Evolution of the 1st Metabolic Cycles, *Proc. Natl. Acad. Sci. USA* **87**(1), 200–204.

Wächtershäuser, G.: 1992, Groundworks for an Evolutionary Biochemistry – The Iron Sulfur World, *Prog. Biophys. Mol. Biol.* **58**(2), 85–201.

Wächtershäuser, G.: 1994, Life in a Ligand Sphere, *Proc. Natl. Acad. Sci. USA* **91**(10), 4283–4287.

Wächtershäuser, G.: 1998, *Thermophiles*, p. 47. Taylor and Francis, Philadelphia.

Wächtershäuser, G.: 2002, Discussing the Origin of Life (comment), *Science* **298**, 748–748.

Will, G., Lauterjung, J., Schmitz, H. and Hinze, E.: 1984, *High Pressure in Science and Technology*, Elsevier, New York.

Yang, W., Parr, R. G. and Pucci, R.: 1984, Electron-Density, Kohn-Sham Frontier Orbitals, and Fukui Functions, *J. Chem. Phys.* **81**(6), 2862–2863.